Food Chemistry: X 25 (2025) 102140

Contents lists available at ScienceDirect

Food Chemistry: X

journal homepage: www.sciencedirect.com/journal/food-chemistry-x

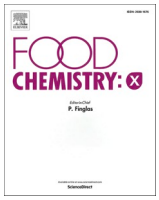

The stabilization mechanism of the pea protein and rutin complex at the gas/liquid interface and its application in low-fat cream

Chunyang Xia [a], Fangxiao Lou [b], Shuo Zhang [b], Tianfu Cheng [b], Zhaodong Hu [b], Zengwang Guo [b,*], Ping Ma [a,**]

[a] College of Food Science, Heilongjiang Bayi Agricultural University, Daqing, Heilongjiang, 163319, China
[b] College of Food Science, Northeast Agricultural University, Harbin, Heilongjiang, 150030, China

ARTICLE INFO

Keywords:
Cream
Foam
Pea protein isolate
Rutin
Interfacial rheology

ABSTRACT

The objective of this study was to substitute partially fat with pea protein isolate (PP)/rutin (Ru) complexes to produce a healthy and stable low-fat whipped cream. Ru enhanced the foam properties of PP. The Ru binding equivalent was the best at a mass ratio of PP/Ru of 64:4, the PP/Ru complexes particle size was the smallest. The synergistic adsorption of Ru reduced the interfacial tension of the complexes and accelerated their diffusion, permeation, and rearrangement at the air/water interface. The results of rheology and Lissajous plots suggested that PP/Ru complexes functioned as an interfacing stabilizer, enhanced the elastic strength of interface film, and improved the stability of foam. PP/Ru complexes as a fat substitute promoted the aggregation of fat globules and the formation of fat globule network structure. When the substitution rate is 10 %, the texture, stability, and microstructure of the sample are nearly identical to those of full-fat cream.

1. Introduction

Fresh cream, when whipped, forms a pliable complex foam system, which is a typical aerated food (Han, Zhu, Qi, Zhang, & Wu, 2023). The plasticity and stability of whipped cream depend largely on saturated fats or hydrogenated oils. In these whipped creams, fat globules coalesce and anchor to the surfaces of bubbles. These anchored fat globules then connect adjacent bubbles by forming aggregated fat chains. This network of connected fat structures creates a solid framework that provides the whipped cream with its firm and stable texture (Hotrum, Stuart, Vliet, Avino, & Van Aken, 2005). Fats typically constitute 30–40 % of the total composition in fresh cream. High concentrations of fats, especially those high in trans and saturated fatty acids, can increase their intake, leading to significant health risks such as elevated LDL cholesterol levels, which contribute to cardiovascular diseases, as well as higher incidences of type 2 diabetes, obesity, and certain types of cancer (Han, Zhu, Zhang, & Wu, 2024). However, reducing fat content often results in textural defects such as roughness, collapse, and shrinkage (Ghribi, Zouari, Attia, & Besbes, 2021). Thus, it is essential to identify appropriate fat substitutes for low-fat creams to address these challenges.

The formation and stabilization of the foam system are crucial to the texture of whipped cream, (Han et al., 2024), thus there is a need to search for new ingredients with excellent foaming properties to serve as fat substitutes. Proteins, with their lower energy density (1–4 kcal/g) compared to fats (9 kcal/g), and good foaming abilities, are commonly used as fat replacers (Zhang et al., 2024). Plant proteins, in particular, offer nutritional benefits, cost-effectiveness, and align with sustainable food production strategies (Han et al., 2024). Pea protein isolate (PP) is a commonly utilized plant protein known for its high availability and diverse functionalities, such as its ability to aggregate. Unlike soy protein isolate, PP does not impart a beany flavor, making it more acceptable in aerated foods. Nevertheless, the dense structure of native PP leads to poor solubility and foaming performance, limiting its application in low-fat cream systems (Guo et al., 2025). Therefore, creating a straightforward method to enhance the foaming performance of PP could increase its applicability in whipped cream products.

Proteins and polyphenols are capable of forming non-covalent complexes via hydrogen bonding and hydrophobic interactions (Günal-Köroğlu, Lorenzo, & Capanoglu, 2023). Extensive research found that the interaction between proteins and polyphenolic compounds could alter protein structures, thereby improving foaming properties.

* Corresponding author at: College of Food Science, Northeast Agricultural University, Harbin, 150030, China.
** Corresponding author at: College of Food Science, Heilongjiang Bayi Agricultural University, Daqing, Heilongjiang, 163319, China.
E-mail addresses: gzwname@163.com (Z. Guo), maping198011@163.com (P. Ma).

https://doi.org/10.1016/j.fochx.2024.102140
Received 20 October 2024; Received in revised form 13 December 2024; Accepted 27 December 2024
Available online 28 December 2024

Dai et al. (2022) demonstrated that tannic acid (TA) altered the conformation and surface hydrophobicity of lactoferrin (BLF), resulting in BLF-TA complexes with improved foam stability. Wen et al. (2023) found that polyphenols could increase the foaming capacity of ovalbumin, with the extent of improvement related to the number and position of hydroxyl groups in the polyphenols. Zhang et al. (2024) used a soy protein isolate-naringenin complex as a fat replacer, producing low-fat cream with a texture similar to full-fat cream. Thus, incorporating polyphenols can significantly improve the formation and stability of protein-based foam systems, enhancing their suitability for low-fat whipped cream applications. However, most studies focus on the macro performance of various protein-based foam systems, such as limit values, foam half-life and foam microstructure (Huang et al., 2024). A deeper understanding of how polyphenol-protein interactions specifically influence the interfacial properties and foam stability under complex processing conditions of foams are still relatively unexplored. This includes the thickness of air-water interface films, viscoelasticity and large amplitude oscillatory shear (LAOS) rheology. Moreover, there is a lack of in-depth investigation into the specific impacts of polyphenol-protein interactions on the morphology and stability of creams, including their effects on fat globule aggregation, and the final cream product's texture. Rutin (Ru), a natural polyphenol presents in tea, orange peels, and tomatoes, exhibits outstanding antioxidant, anticancer, and anti-inflammatory properties (Zhao et al., 2024). Among them, the strong antioxidant activity of rutin is not only beneficial for health, but also plays a crucial role in stabilizing PP. Specifically, rutin helps protect the fat and protein in whipped cream from oxidative degradation, effectively preventing negative impacts on the flavor, texture, and overall quality of the product. By reducing the oxidation process, rutin can help extend the shelf life of plant-based whipped cream, which is crucial for maintaining the quality and stability of low-fat whipped cream systems. Hence, PP/Ru complexes can hold great potential as fat replacers in low-fat whipped cream systems.

In this study, we investigated how PP/Ru complexes at various mass ratios can stabilize low-fat whipped cream, focusing on the relationship between structure, air/water interface behavior, foam properties, and low-fat cream texture. We analyzed the structural properties of these complexes using polyphenol binding equivalents, particle size, and zeta potential measurements. Their adsorption behavior at the air/water interface was examined through interfacial dilatational rheology. The foam characteristics were assessed by microstructure and shear rheological properties. Additionally, we prepared low-fat whipped cream using PP/Ru complexes as a fat replacer and evaluated its stability by monitoring appearance changes, fat aggregation rate, hardness, and microstructure. This comprehensive approach provides valuable insights into the effective use of PP/Ru complexes as plant-based fat replacers in low-fat whipped cream, supporting the rational design of future food formulations to enhance product quality and stability while promoting healthier fat alternatives.

2. Materials and methods

2.1. Materials and chemicals

PP (88.3 % crude protein, based on dry weight) was purchased from YUWANG ECO Co., Ltd. (Shandong, China). Ru (purity ≥95 %) was purchased from Pusi Bio-Technology Co., Ltd. (Chengdu, China). All other chemical agents were of analytical grade, which were purchased from Sinopharm Chemical Reagent Co., Ltd. (Shanghai, China).

2.2. PP-Ru complexes preparation

The PP solution (5 mg/mL) was mixed with a 0.01 % (*w/v*) Ru stock solution at mass ratios of 64/0, 64/1, 64/2, 64/3, 64/4, and 64/5. The mixture was stirred at room temperature (25 °C) and a speed of 500 rpm for 2 h. Finally, the final concentration of PP and the pH in the mixed solutions were 0.1 % and 7.0, respectively.

2.3. Polyphenol bound equivalents

In brief, a 1 mL aliquot of the sample was mixed with 1 mL Folin–Ciocalteu reagent (0.25 mol/L). Following a 5 min incubation, 2.0 mL of a 15 % (*w/v*) Na_2CO_3 aqueous solution was added. After standing at 25 °C for 30 min under shaking and dark conditions. The absorbance of the supernatant was measured at 760 nm using a Unico 2100 spectrophotometer (Unico Co., Shanghai, China). The Ru content was calculated from the calibration curve and final results expressed as nmol/mg (Li et al., 2015).

2.4. Particle size and ζ-potential

Before conducting particle size and ζ-potential analysis, the sample was diluted to 0.01 % (w/v) of protein in a phosphate buffer. The Zeta Sizer Nano ZS90 (Malvern, U.K.) was used to measure samples at 25 °C. The refractive indexes for the protein particles and the dispersion medium were 1.46 and 1.33, respectively.

2.5. Foam morphology

Real time monitoring of bubble size change in PP/Ru composite system by dynamic foam analyzer (DFA100, KRUSS, Germany).

The microstructure of foams was observed using a Confocal Laser Scanning Microscope (CLSM) (LSM880, Carl Zeiss, Germany). The composite solution was labeled with 0.02 % Rhodamine B, and then it was made into foam. Finally, the image was observed with an excitation wavelength of 540 nm with 10 × objectives, where red represents proteins.

2.6. Interfacial tension

The adsorption behavior at air-water interface was studied by a Tracker Automatic Drop Tensiometer (Teclis, France). Using a glass syringe, 6 mL of the sample solution was drawn up, and then a rising bubble with a volume of 15 mm^3 was produced at the tip of a J-shaped needle, which was then allowed to equilibrate for 2 h. The shape of the bubbles over time was recorded using a camera, and the interfacial tension was calculated by fitting the data with the Young-Laplace equation.

2.7. Interfacial dilatational rheology

After equilibration for 2 h, the bubble was oscillated with an amplitude of 5 % to 40 % and a frequency of 0.02 Hz. According to the method developed by Sagis and Fischer (2014), rheological information of the sample was obtained through Lissajous figures. The relationship between surface pressure and deformation extent was obtained according to the formula (S(t)-S0)/S0.

Where S(t) denotes the area of the bubble at time t, and S0 stands for its initial undeformed area.

2.8. Interfacial shear rheology

The rheological properties of the foam were measured using an RS6000 rheometer (Haake, Germany) at 25 °C. In the amplitude sweep, the amplitude was increased from 0.001 % to 100 % at frequency of 1 Hz. In the frequency sweep, the frequency was increased from 0.1 Hz to 10 Hz at the strain of 0.5 %.

2.9. Preparation of creams

The preparation of the samples was carried out according to the method described by Zhang et al. (2024). Full-fat cream was composed

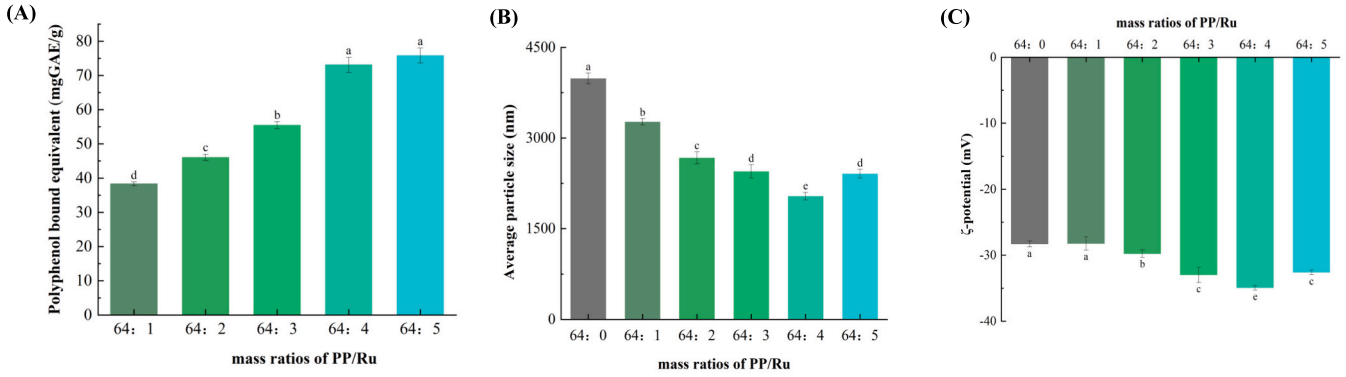

Fig. 1. The percentage content of polyphenol binding (A), average particle size (B), andζ-potential (C) in PP/Ru complexes with different mass ratios.

of 25 % hydrogenated palm oil, 1.08 % sodium stearoyl lactate, 15.02 % white sugar, 7.51 % sucrose syrup, 0.95 % D-sorbitol and 0.18 % xanthan gum. Finally, used water to make up to 100 %. The PP/Ru complexes with a mass ratio of 64:4 was used to replace fat in cream, and at different substitution levels (5 %, 10 %, 15 % and 20 %), low sugar creams were named as C-PP/Ru-5 %, C-PP/Ru-10 %, C-PP/Ru-15 % and C-PP/Ru-20 %, respectively. The low-fat cream prepared by replacing 10 % fat with PP was named C-PP-10 %.

2.10. Fat partial coalescence rate (Φ)and overrun

The mixture consisting of 20 g of cream and 10 g of Oil Red O dye was centrifuged at 10000 ×*g* for 30 min at 25 °C. Soybean oil without Oil Red O was used as the control, and the absorbance of the dye solution was measured at 520 nm. The calculation was performed according to the following equation:

$$\Phi(\%) = \frac{M_1 \times (\alpha - 1)}{M_2 \times \Psi} \times 100 \quad (1)$$

where M_1 (g) represents the mass of added Oil Red O solution. α is the ratio of absorbance of Oil Red O solution before and after centrifugation. M_2 (g) and Ψ (*w*/w%) are the mass of cream and the mass fraction of fat, respectively.

The calculation formula for Overrun is as follows:

$$\text{Overrun}(\%) = \frac{m_1 - m_2}{m_2} \times 100 \quad (2)$$

where m_1 (g) is the mass of unwhipped sample, and m_2 (g) is the mass of whipped sample (g).

2.11. Cream stability

The whipped cream was shaped into a rose flower form, and changes in its appearance were recorded using a digital camera at 0 and 8 h.

The cream texture (hardness, consistency and cohesiveness) was measured using texture analyzer (Stable Micro System Co., London, U. K.). The trigger value was 5.0 g.

2.12. Confocal laser scanning microscopy

After dilution, 0.5 mL of the cream sample was thoroughly mixed with 20 μL of Nile Red and 20 μL of Nile Blue solution. The mixture solution was then stained in the dark for 30 min. Subsequently, the sample was placed on a slide for observation using CLSM.

2.13. Statistical analysis

Each experiment was repeated three times, and the results are reported as mean ± standard deviation. Statistical significance was detected by Tukey's multiple-range test ($p < 0.05$) utilizing the IBM SPSS Statistics 20 (SPSS, Inc., Chicago, IL, USA).

3. Results and discussion

3.1. Polyphenol bound equivalents of PP/Ru complexes analysis

To determine the carrying capacity of PP for Ru, the unreacted Ru in the samples was removed through dialysis. Using polyphenol bound equivalents to express the successful combined polyphenol content. This could help elucidate the stability mechanism of PP/Ru complexes at the gas-liquid interface, as the extent of Ru binding to PP can influence the structure and functionality of PP. Fig. 1(A) illustrates the effect of noncovalent interactions between PP and Ru on the polyphenol binding equivalent. The amount of Ru bound to PP significantly increased as the mass ratios of PP/Ru increased. The increase in the amount of bound Ru was no longer significant above 64:4. This saturation phenomenon was primarily due to the Ru concentration reaching or exceeding the number of binding sites on the PP side chains, which may be provided by the amino or thiol side chains (Dai et al., 2024). Notably, the number of active sites in PP may be influenced by its structure changes as the reaction proceeds.

3.2. Particle size and ζ-potential of PP/Ru complexes

Particle size and ζ-potential can affect the formability, stability and shape of the foams and bubbles (Fujii, 2024). Because particle size largely determines the rate of particle adsorption and diffusion of protein particles at the air/water interface, and the electrostatic interaction is one of the factors affecting the arrangement of protein particles on the interface film. As illustrated by Fig. 1, the mass ratios of PP/Ru affecting the particle size of PP/Ru complexes (Fig. 1B) and ζ-potential (Fig. 1C). Although there might be a misconception that binary complexes form larger particle sizes compared to single proteins, the reality is actually the opposite. The average particle diameter of PP/Ru complexes significantly decreased compared with the plain PP and showed a trend of decreasing and then increasing with the increase of the mass ratios. The hydrophobic effect and the more compact structure could be resulted in the reduced size of the PP/Ru complexes (Najari, Dokouhaki, Juliano, & Adhikari, 2024). Indeed, a previous study reported that particles with smaller sizes require less energy to overcome adsorption energy barriers during the adsorption process, thus being conducive to their adsorption at the interface (Cheng et al., 2024). Moreover, the ζ-potential of all the samples was negative owing to the negative charge on the surfaces of the PP molecules above the isoelectric point. The absolute ζ-potential of PP increased after noncovalent binding with Ru, suggesting greater electrostatic repulsion between PP molecules, which

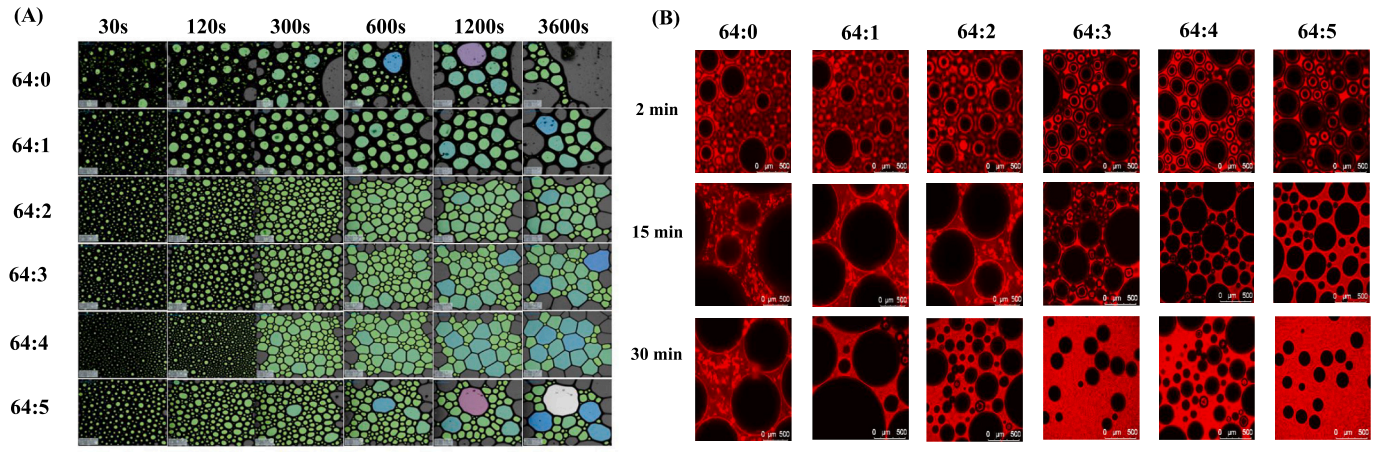

Fig. 2. Time evolution of the bubbles stabilized by PP/Ru complexes with different mass ratios; (A) microstructure images; (B) CLSM image.

was also found in Tian et al. (2023). The increase in the absolute ζ-potential values may occur for two reasons. First, this could be attributed to changes in the secondary structure of PP and the extension of the PP structure caused by Ru, resulting in a reduction in the exposure of positively charged groups and an increase in the negative charge. Second, the formation of hydrogen bonds between PP and Ru led to the deprotonation of the hydroxyl groups in the polyphenols, thus generating oxygen centers with a high negative charge density (Rodríguez, von Staszewski, & Pilosof, 2015). However, when the mass ratio of PP to Ru exceeds 64:4, excess polyphenols that are weakly bound to the surface of protein molecules may form a metastable network structure (Han et al., 2023). At this point, the polyphenol binding equivalents stabilize and no longer increase, thus disrupting the original stability of the system. The absolute ζ-potential of PP/Ru complexes significantly decreased. The PP may undergo aggregation to result in an increase in particle size.

3.3. Microscopic foam morphology

Fig. 2A shows the microstructure images of foams stabilized by PP/Ru complexes with various PP/Ru ratios. Initially, all samples formed small, spherical bubbles. Over time, the bubble size of the foams increased gradually due to the combined effects of foam coalescence and disproportionation (Chen et al., 2019). This was because all the foams were thermodynamically unstable, possessing high surface free energy at the air-water interface. Alternatively, Alternatively, gravity caused the liquid at the air-water interface to be expelled into the plateau border channels by capillary forces (Chen et al., 2019). This caused foam instability, reducing interface film thickness and leading to foam coalescence and increased size. The foam produced by the PP/Ru complexes was smaller and more abundant than that of the control. And it is especially the foam stabilized by the PP/Ru complexes with PP/Ru ratios of 64:4. After recording for 20 min, the increase rate of bubble size of PP/Ru complexes with PP/Ru ratios of 64:2, 64:3, 64:4 seems to be slower. Moderate amounts of Ru can enhance foam stability by reducing the gas-liquid interfacial tension of PP or improving the viscoelasticity of the liquid film. These results proved that PP/Ru complexes were more effective in stabilizing foams.

This work introduces PP/Ru complexes as fat substitutes to explore their impact on the performance of low-fat cream that is an aerated food. Therefore, employing CLSM is essential for observing the adsorption and accumulation of complexes on the bubble surface. The CLSM images of the foams stabilized by PP/Ru complexes with different Ru concentrations and PP alone were recorded in Fig. 2B, where the protein is marked in red. The shell structure surrounding the bubble surface was distinctly visible in all samples. This indicated that both PP and PP/Ru complexes could efficiently diffuse to and adsorb at the air-water interface, subsequently forming an aggregated interfacial film. Compared with the foams stabilized by single PP , the foam interface formed by PP/Ru complexes shows the bilayered structures. An additional hydration layer

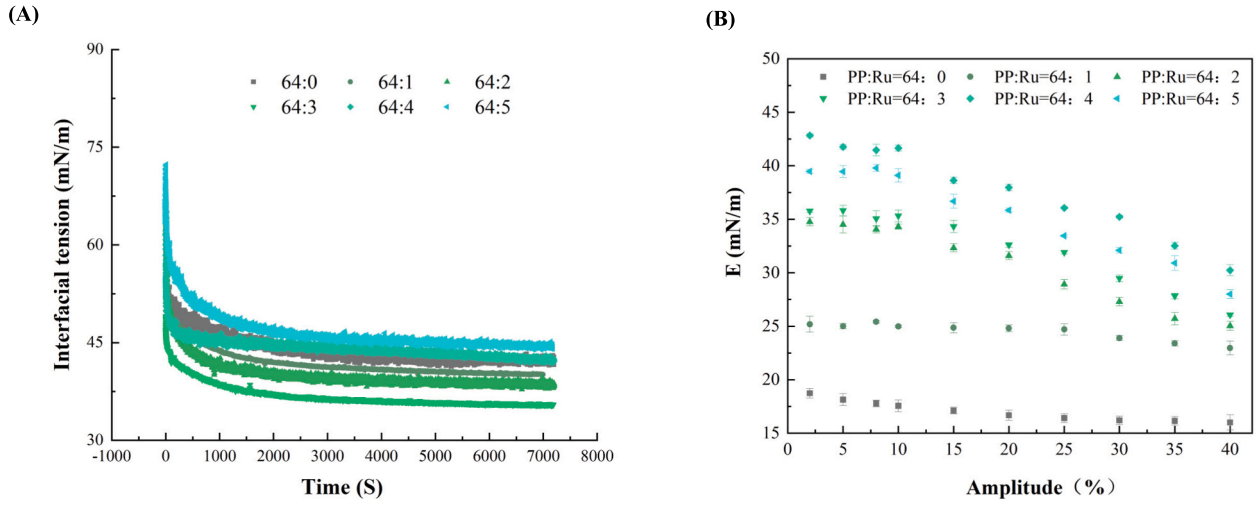

Fig. 3. Interface tension of adsorption (A) and amplitude sweeps (B) of different mass ratios of PP/Ru at the air/water interface.

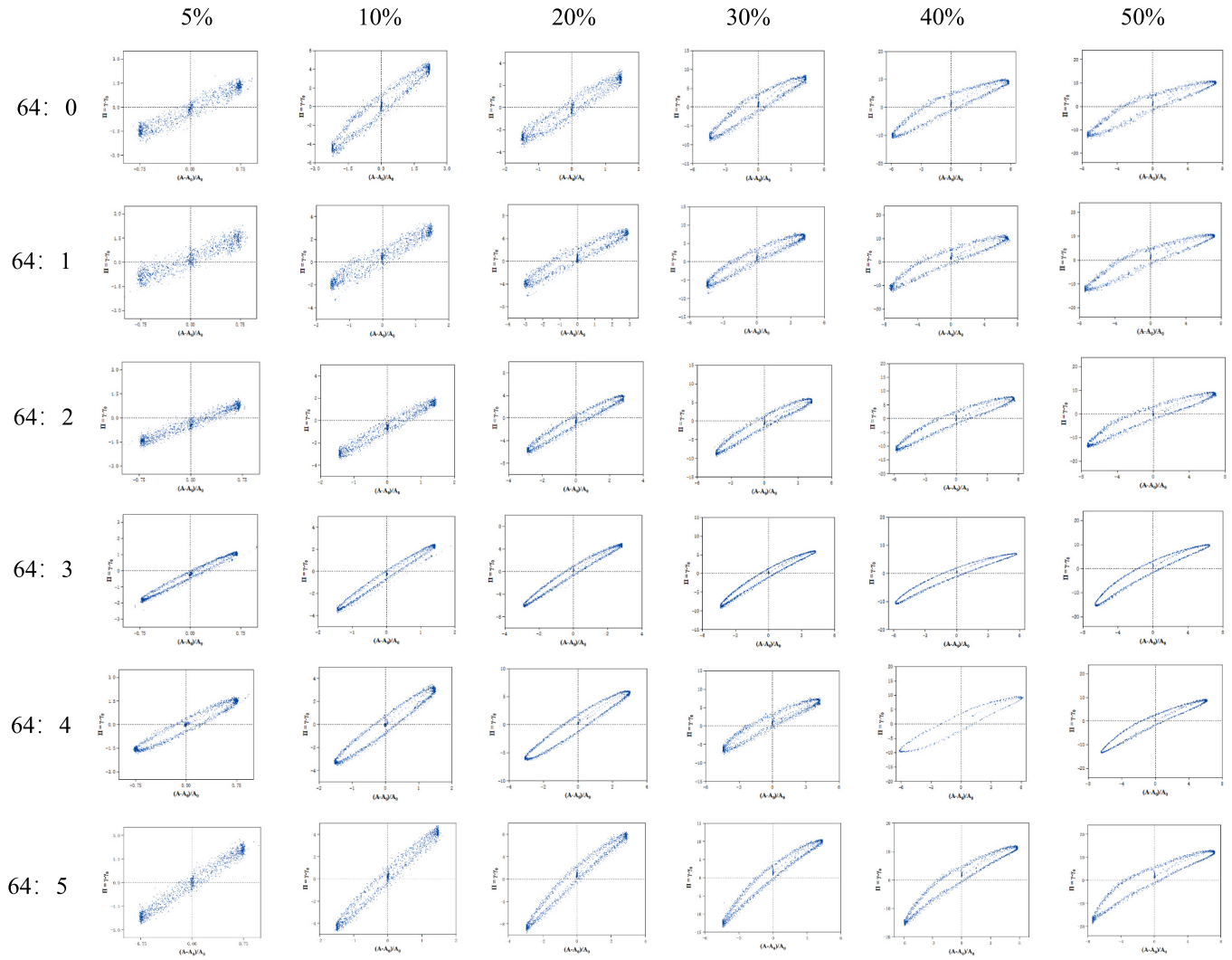

Fig. 4. Lissajous curves of different mass ratios of PP/Ru at the air/water interface.

(outer black ring) was formed, at the protein layer periphery, and the thickness of the hydration layer was Ru concentration-dependent enhancement. This could be associated with the rearrangement of PP molecular conformation during the binding process between Ru and PP. The abundant hydrophilic groups may be more exposed on the surface of PP, such as $-NH^{3+}$, $-COO^{-}$, −OH, −SH, etc. These hydrophilic groups were prone to hydration, forming a thick hydration layer around the protein layer (Mallamace et al., 2015). After 10 min of standing, large bubbles formed in the PP group, even beyond the microscope's field of view. The amount of PP adsorbed on the interface layer significantly decreases, and more PP aggregates were displayed in its continuous phase, indicating that the foam's liquid dissipated more rapidly in the PP group due to disproportionation and coalescence. By contrast, the interface layer formed by PP/Ru complexes was thicker, the foam was stable and not prone to aggregation, especially when the the mass ratios of PP/Ru was 64:4. This implies that the Ru can effectively enhance the dispersion of PP molecules and sorption capacities at the air–water interface (Wang et al., 2024). The adsorbed PP/Ru complexes enhance the elasticity of the interfacial film, forming a more stable kinetic and steric structural barrier (Xu et al., 2021). It effectively prevents bubble shrinkage and gas diffusion, thereby enhancing foam stability.

3.4. Interfacial tension

The interfacial behavior of protein-polyphenol complexes has a significant impact on their foaming properties. This article evaluates the influence of interfacial behavior on the foaming performance of PP and PP/Ru complexes by measuring their dynamic interfacial tension at the air-water interface. Generally, proteins, as high molecular weight surfactants, have multiple anchoring sites at the interface. Therefore, its interfacial adsorption behavior includes three stages of protein diffusion, permeation, and structural rearrangement from the aqueous phase to the gas phase surface. Meanwhile, the gradually adsorbed protein molecules rapidly grow under adsorption and gradually reach an equilibrium state, thereby stabilizing the interfacial layer. This behavior influences the rheological characteristics of the interface and the adsorption layer of fixed proteins (Wu, Feng, Wang, Zhang, & Wang, 2023). As shown in Fig. 3A, the dynamic surface tension curves of all samples show a similar trend of change. The dynamic interfacial tension decreases with increasing measurement time, but the magnitude of the decrease is relatively small. This suggests that complexes particles persistently adsorb at the interface until equilibrium is achieved. In PP/Ru complexes systems with different concentrations, the interaction between Ru and PP changes the conformation of the gas/liquid surface adsorption layer, thereby altering the interfacial tension of the solution. Compared with PP, PP/Ru complexes with mass ratios of 64:1, 64:2, and 64:3 significantly reduced their surface tension. This is mainly because Ru has a synergistic adsorption effect on PP, promoting the interfacial adsorption of PP/Ru. In addition, Ru interacts with protein nanoparticles, aiding in protein structure relaxation and dissociation, which

facilitates its unfolding and rearrangement at the two phases interface. This change endows the interface adsorption layer with better flexibility and fluidity, accelerating the diffusion, permeation, unfolding, and rearrangement of the complexes at the interface, providing better macroscopic foaming ability. On the other hand, Ru accumulates on amino acids' hydrophobic side chains, disrupting the hydrophobic-hydrophilic residue balance. Enhanced hydrophobicity increases the complex's adsorption rate at the interface, thus potentially improving the sample's foaming performance (Ye et al., 2021). At the same time, Ru acts as a "bridge" between proteins, enhancing the connection between protein molecules. This results in a higher interface density, which improves the system's stability against external deformation effects (Wu et al., 2024). However, PP/Ru complexes with higher quality (64:4, 64:5) have longer adsorption times and increased surface tension. This may be due to excessive modification of PP by Ru, resulting in hydrophobic amino acids participating in protein binding. This will reduce surface interactions and generate large and complex aggregates, reducing adsorption rate and delaying interfacial equilibrium time. However, the interfacial surface tension alone is inadequate for predicting a solution's foaming characteristics. Therefore, this study thoroughly examined the relationship between the solution's air/water interface behaviors and foam performance.

3.5. Interfacial dilatational rheology

3.5.1. Amplitude sweeps

The stability of foam depends largely on its interfacial rheological properties. In essence, the interface with high viscoelastic modulus and strong mechanical properties has excellent foam stability. In order to further investigate the interfacial rheological properties, oscillatory expansion deformation experiments (with amplitudes ranging from 2 % to 40 %) were conducted on droplets that reached equilibrium after adsorption. The linear viscoelastic region can be determined by amplitude scanning, and the correlation information between the interfacial expansion viscoelastic modulus and amplitude can be obtained by amplitude scanning (Kontogiorgos & Prakash, 2023). Fig. 3B shows the variation curve of the interfacial expansion dilatational viscoelastic modulus with amplitude. As shown in the figure, when the amplitude range is 2 % to 10 %, the dilatational viscoelastic modulus of all samples does not change much with the applied amplitude, indicating that 2 % to 10 % is the linear viscoelastic region of all samples. When the amplitude is greater than 10 %, we observed that the dilatational viscoelastic modulus) of all complexes stable interfaces decreases with the increase of amplitude. This results from significant deformation of the interface microstructure, causing the interface film structure to break down. The PP/Ru complexes exhibit a lower rate of decrease in elastic modulus than a single PP system when the amplitude is greater than 10 % (belonging to nonlinear deformation). This change means that the interaction between interface proteins has a significant impact on the interface structure. During the period of oscillatory deformation, the active molecules on the interface undergo structural reorganization (Murray, Ventura, & Lallemant, 1998). The research shows that the interaction between adsorbed molecules on the interface is enhanced after adding Ru, thus forming a more elastic interface film. This change makes it show higher foam stability at the macro level. The specific changes in nonlinear rheology were further discussed through the Lissajous plots.

3.5.2. Lissajous plots

To further analyze the linear and nonlinear rheological behaviors of PP/Ru stabilized air-water interfaces in the small and large deformations regime, Lissajous plots were constructed (Sun et al., 2025). As shown in Fig. 4, the Lissajous plot's shape is significantly influenced by deformation magnitude and variations in Ru concentration. Lissajous plots exhibit a clockwise closed loop under applied deformation, with the plot's upper section indicating interface extension and the lower section representing compression. The graph between extension and compression could reflect the rheological type of the interface layer. Lissajous plots depict the state of interfacial films, with linear and circular shapes indicating elastic and viscous behaviors, respectively, and elliptical shapes representing viscoelastic properties. Axisymmetric ellipses suggest a linear viscoelastic response, while asymmetric ellipses indicate a nonlinear response. The asymmetry of the plots indicates interactions among adsorbed molecules. In addition, the angle between

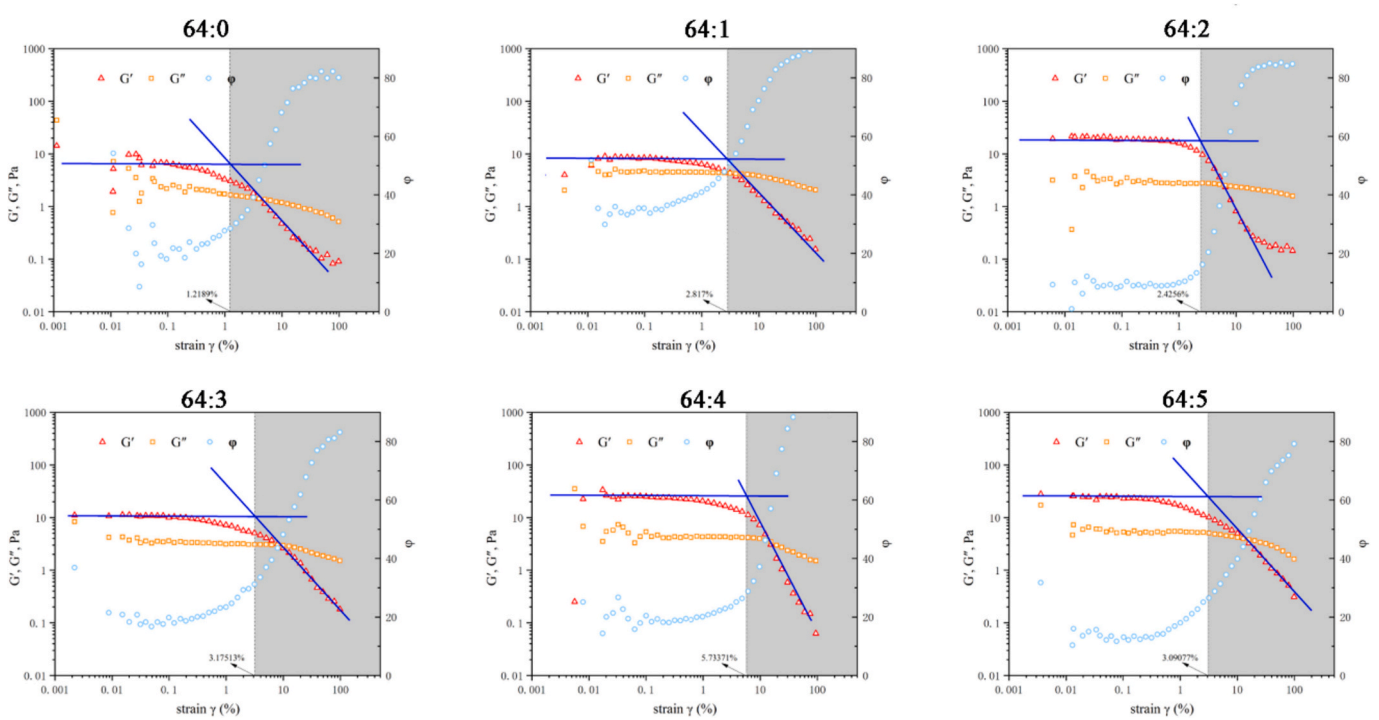

Fig. 5. Functional relationship between viscous/elastic modulus (G' and G") and strain of foam prepared by PP/Ru complexes with different mass ratios.

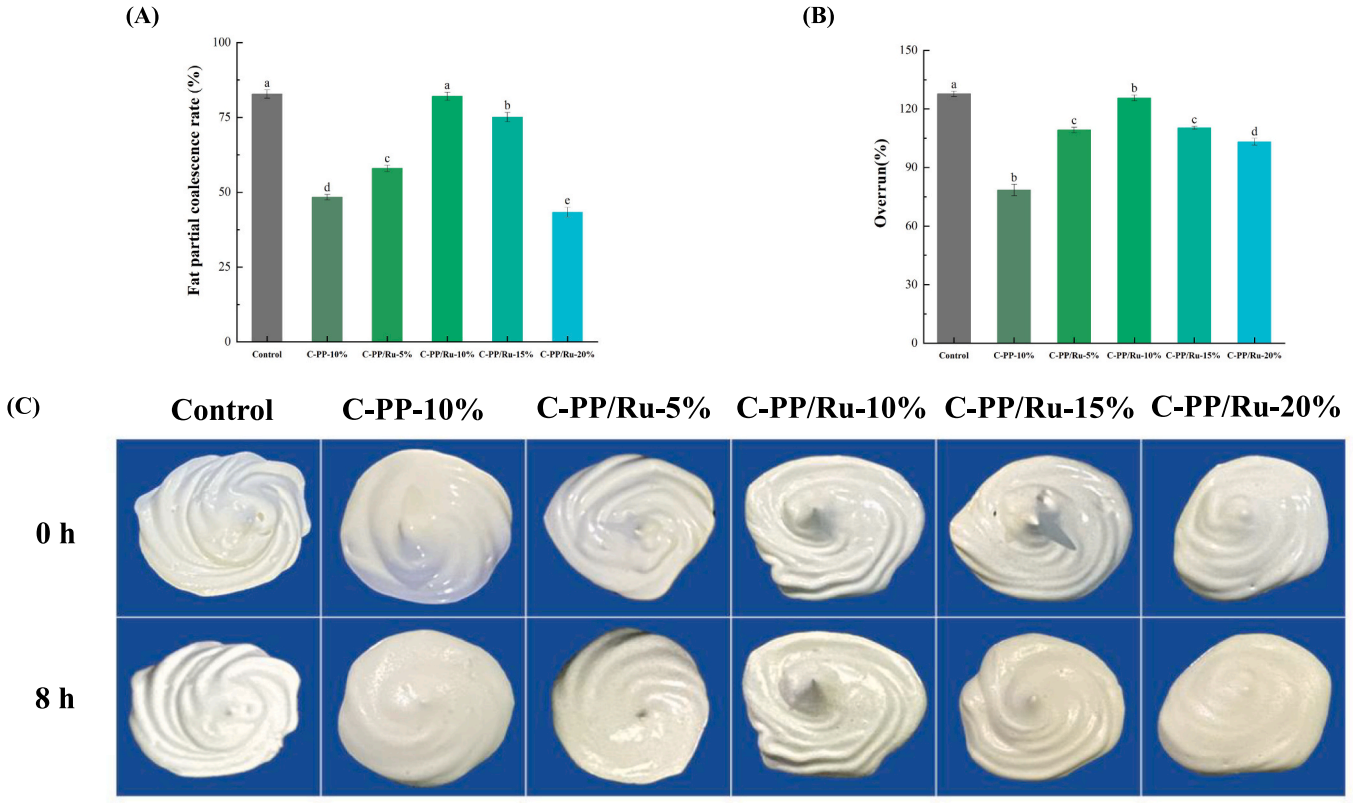

Fig. 6. Fat partial coalescence rate (A), overrun values (B), mounting performance (C) of whipped cream made from whole fat, C-PP-10 %, and PP/Ru complexes with different substitution ratios.

the plots and the horizontal axis is significant for interfacial mechanics. A plot with a steeper slope indicates increased interface stiffness. For PP sample, the Lissajous plots is a narrow symmetric ellipse, indicating the linear viscoelastic behavior. PP/Ru complexes with varying mass ratios at the air/water interface exhibited enclosed areas in their Lissajous plots at amplitudes of 10 % to 20 %, demonstrating a linear viscoelastic response characterized by an approximately axisymmetric ellipse. As deformation increased, the Lissajous plots expanded and became asymmetric, indicating interface structure disruption at higher amplitudes. Besides, the Lissajous plots exhibit considerable noise, likely due to the adsorption rate of the samples at the interface being substantially lower than the bubble deformation rate under small amplitude conditions. As interfacial deformation increases during the extension process, the slope of the Lissajous plot decreases, indicating strain softening of the interfacial film. Furthermore, during the compression process, the Lissajous plot's slope progressively rises with increased interfacial deformation, indicating strain stiffening of the interfacial film (Niu et al., 2023). The degree of this phenomenon will intensify with the increase of amplitude. As the concentration of Ru increases, the degree of expansion softening and strain hardening gradually increases. In addition, under the same amplitude, the width of the Lissajous plot at the interface of PP/Ru complexes initially increases and then decreases as the Ru addition increases. It meant that the strain-softening during extension results from the disruption of interfacial structure and decreased protein density. The strain-hardening during compression likely arises from the jamming of the interfacial structure, leading to a significant increase in protein density and interactions (Huang et al., 2021). Analysis of Lissajous plots revealed that a PP/Ru ratio of 64:3 resulted in narrow elliptical shapes and a quicker elastic response in the interface layer. This is primarily attributed to Ru's strong hydrophobicity and high positive charge, which facilitate interfacial anchoring and intensify protein-protein hydrophobic interactions, thereby enhancing lateral interactions among interfacial macromolecules. This will enhance the rapid adsorption ability of PP/Ru complexes at the air-water interface, thereby filling the interface layer and forming the interfacial structure with higher elastic network. This aids in enhancing foam stability. At a PP/Ru ratio of 64:5, the Lissajous plots became wider, and a pronounced strain hardening effect was measured. This was due to the predominant adsorption of Ru when a substantial amount was added. This will reduce protein density, resulting in the weakest deformation. To sum up, the moderate addition of Ru leads to the formation of a highly elastic interface structure in the PP/Ru complexes system.

3.6. Strain sweeps

The rheological properties of foam depend on the size, deformation and mechanical properties of foam. The strain sweeps can not only characterize the stability of foam from the aspects of structure and properties, but also determine the linear viscoelastic region of foam. The storage modulus (G′) and loss modulus (G″) represent the contributions of elasticity and viscosity, respectively (Cheng et al., 2024). The viscoelastic properties of foam prepared by PP and PP/Ru complexes with different concentrations are evaluated by strain sweeps. As strain increases, two distinct regions were distinguished: the linear viscoelastic region, where G′ and G″ remained nearly constant, and the nonlinear region, where both ′ and G″ began to decrease. As shown in Fig. 5, G′ remains constant until reaching a critical strain point, after which it decreases sharply. The critical strain (γc) is defined by the strain when G′ starts to decline sharply, reflecting the ability of foam to resist strain. When the critical strain (γc) is reached, the foam enters the nonlinear viscoelastic region. In the linear viscoelastic region, the elastic modulus is higher than the viscous modulus at all foam systems, which indicates that all foam samples may have a weak gel network structure. The foam prepared with PP/Ru complexes exhibits higher G′ and G″ values

compared to foam made solely with PP. In particular, when the mass ratio of PP/Ru complexes is 64:4, the foam shows the highest G′ and G″ values and γc. This result may be due to the moderate Ru concentration fostering deeper penetration and rearrangement of complexes at the interface, thus aiding in the formation of a stable viscoelastic interfacial film. This will increase the strength of the internal structure of the foam system, which can be used to resist deformation in complex processing environments (Guo et al., 2025). In addition, the foam prepared by PP/Ru complex with a mass ratio of 64:4 enters the nonlinear region with a larger strain, indicating that the foam has better stability. Under high shear strain, spherical bubbles break into smaller bubbles and align with the shear direction. As a result, the moderate quality ratio of PP/Ru enhanced the foam structure's resistance to shear stress.

3.7. Characterization of creams

3.7.1. Fat partial coalescence rate and overrun

The incomplete coalescence of fat is the key factor affecting the structure and stability of foam during whipping. Generally, a higher rate of fat partial coalescence is beneficial for forming a stronger foaming system (Allen, Murray, & Dickinson, 2008). Under this condition, the cream has better overrun. In general, higher whipped cream overrun enhances foam structure and improves cream quality. The rate of fat partial coalescence whipped cream made from PP/Ru complexes at different substitution rates are shown in Fig. 6A. The fat partial coalescence rate of C-PP-10 % showed a significant decrease compared to the control. This may be because the functional properties of PP are poor and the bubble film adsorbs a small amount of PP, which cannot promote the coalescence of fat. Meanwhile, the rigid protein structure impedes the connection of fat globules, reducing the rate of partial coalescence. In addition, the fat coalescence rate of whipped cream made from PP/Ru complexes with varying substitution rates was significantly higher than that of C-PP-10 %. This may be because PP modified by Ru has better amphiphilicity. They can be adsorbed to the surface of the bubble film faster, and the bubble film is more viscoelastic, so that more fat globules can be adsorbed and coalesced. However, when the substitution rate exceeds 10 %, the content of PP/Ru complexes adsorbed by the fat globules increases and the fat globule membrane becomes too stable. Consequently, crystalline fat struggles to penetrate the surface of fat globules, making it difficult for fat to coalesce (Huyst et al., 2023).

Fig. 6B illustrates that the overrun of cream exhibits a trend comparable to the rate of fat partial coalescence. The overrun of C-PP-10 % showed a significant decrease compared to the Control. This may be because the rigid PP likely impedes fat globule aggregation, resulting in a discontinuous fat globule network. They cannot prevent gas from escaping, resulting in a decrease in overrun. Compared with C-PP-10 %, the overrun of C-PP/Ru-10 % is significantly increased. This may be because the modified PP structure is more expanded. They rapidly adsorb onto bubble surfaces, facilitating partial coalescence of fat globules. Furthermore, PP/Ru complexes, as a component of the fat globule network, forms a strong fat globule network to wrap bubbles, resulting in an increase in overrun (Goff, 1997). When the substitution rate exceeds 10 %, the fat content decreases. The rates of fat globule coalescence and network structure formation in cream have both decreased. This hinders the formation of a dense and stable fat globule network, making it impossible to retain too much gas, resulting in a decrease in overrun.

3.7.2. Cream stability

Cream is typically consumed shortly after production, so the short-term form stability of cream (a few hours) directly affects people's acceptability of it. The short-term shape retention ability of whipped cream made from PP/Ru complexes at different substitution rates can be evaluated by its rosette-like appearance changes and degree of collapse at different storage times (Liu et al., 2022). From Fig. 6C, it can be clearly seen that full-fat cream has sharp edges, firm peaks and clear textures. After 8 h, the texture of the full-fat cream is still clear and the firm state is good. On the contrary, C-PP-10 % cannot show a rosette-like structure due to its rapid collapse, resulting in a rough surface and the generation of many bubbles. After 8 h, the C-PP-10 % texture almost disappeared. Interestingly, the contour clarity of whipped cream can almost be compared to full-fat cream when the PP/Ru complexes substitution rate is 10 %. This may be because the PP/Ru complex adsorbed to the interface film can form a protein protective layer that stabilizes the bubble structure inside the cream (Liu et al., 2022). However, when the substitution rate exceeds 10 %, the protein content further increases, and the number of fat globules further decreases. This decreases the likelihood of fat globule collisions, hindering the formation of a continuous fat crystal network and resulting in the cream's inability to stand.

Table 1
The textural properties of whipped cream made from whole fat, C-PP-10 %, and PP/Ru complexes with different substitution ratios.

Samples	Hardness/g	Consistency/g.s	Cohesiveness/g
Control	282.32 ± 0.83^{c}	1885.76 ± 21.08^{e}	33.39 ± 0.17^{d}
C-PP-10 %	197.45 ± 1.56^{d}	1400.54 ± 54.06^{f}	18.54 ± 0.56^{e}
C-PP/Ru-5 %	207.39 ± 1.65^{d}	2056.78 ± 32.02^{d}	56.78 ± 0.45^{c}
C-PP/Ru-10 %	283.28 ± 1.17^{c}	3354.45 ± 33.02^{c}	64.54 ± 0.31^{b}
C-PP/Ru-15 %	500.49 ± 0.78^{b}	4099.45 ± 56.07^{b}	65.49 ± 1.78^{b}
C-PP/Ru-20 %	550.81 ± 1.24^{a}	4234.89 ± 31.09^{a}	74.54 ± 0.43^{a}

All the data are expressed as mean ± SD. Means with the different superscript letters within the same column for each parameter are significantly different ($P < 0.05$).

3.7.3. Texture

Hardness, consistency and cohesiveness are the main evaluation indexes for cream texture. The results for the texture properties of cream are shown in Table 1. Generally, cream is too soft and collapses easily, and too hard and is difficult to mold. The hardness of whipped cream stabilized by PP is significantly lower than that of whipped cream stabilized by PP/Ru complexes at the same substitution rate. This is because the spherical structure of PP molecules is not completely unfolded, hindering crosslinking with other substances in the liquid phase (Muse & Hartel, 2004). However, the addition of Ru can induce the structural expansion of PP, and the internal groups of PP molecules are fully exposed, resulting in a significant increase in the intermolecular bridging probability. Notably, there is no significant difference in hardness between whipped cream with PP/Ru complexes substitution rate of 10 % and full-fat cream. Furthermore, the hardness of whipped cream rises as the substitution rate of PP/Ru complexes increases. This is mainly due to the fact that protein is able to provide an elastic and sturdy texture compared to liquid fat, thus increasing the overall hardness of the cream (Han, Zhu, et al., 2023). Similarly, the results of consistency and cohesiveness were consistent with the results of hardness. Consistency and cohesiveness of cream samples increased significantly with addition of PP/Ru. During the whipping process, the partially crystallized fat globules and unstable fat globules tend to move towards the foam interface. Under shearing, the fat globules are locally fused to form a cross-linked network to stabilize the foam. Meanwhile, the emulsion also transitions from a viscous state to a viscoelastic solid state, ultimately resulting in a better texture of the cream. Overall, the addition of PP/Ru led to higher textural properties for low-fat cream, which also meant that the low-fat cream supplemented with PP/Ru had a denser fat globule network structure.

3.7.4. Microstructure of whipped cream

Confocal laser scanning microscope can directly observe the distribution of fat (green area) and protein (red area) in whipped cream made of PP/Ru complexes at different substitution rates (Wang et al., 2023). It can be clearly seen from Fig. 7 that the fat distribution in full-fat cream is

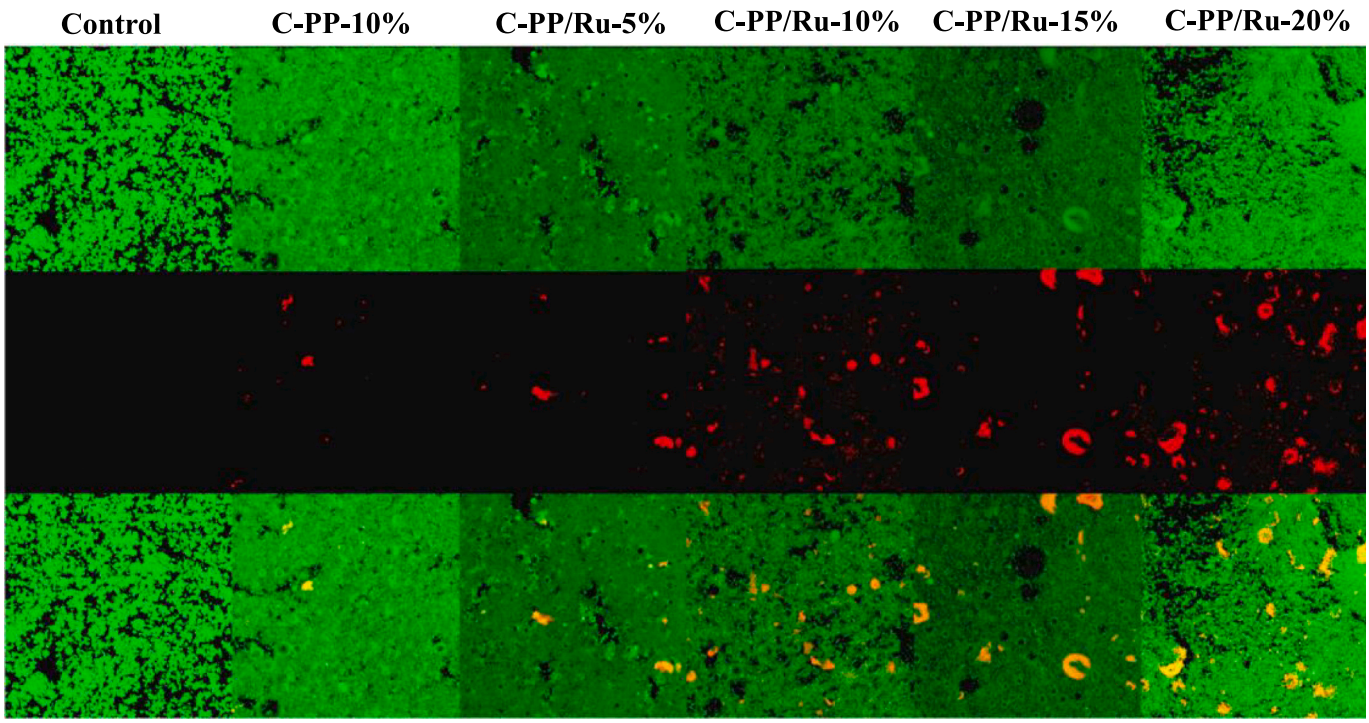

Fig. 7. CLSM images of whipped cream made from whole fat, C-PP-10 %, and PP/Ru complexes with different substitution ratios.

dense, forming a uniform pore distribution dominated by small pores. However, C-PP-10 % exhibits minimal fat coalescence and contains a low content of interfacial membrane protein. This could be due to the lower adsorption of PP in C-PP-10 % on the bubble film, which prevents the fat network structure from stabilizing the foam during the cream whipping process, thus reducing the stability of whipped cream (Dickinson, 2017). Compared with C-PP-10 %, the degree of fat coalescence and the content of interfacial membrane protein in C-PP/Ru-10 % were significantly increased. This may be because the PP/Ru complex has good emulsifying properties and the PP/Ru complex acts as a component of the interface film in the aerated whipped emulsion system. They can form a good viscoelastic interface film in the whipping cream system, thus playing a role in protecting foam. Meanwhile, the affinity between PP/Ru complexes and fat also promotes the formation of a network structure of fat molecules. However, when the substitution rate is less than 10 %, the interface proteins are unevenly distributed and some adsorbed proteins form a protective layer of fat clusters, ultimately forming a discontinuous fat globule network. When the substitution rate is higher than 10 %, the content of interfacial protein increases, but the content of fat globules is too low. Proteins create a barrier on the bubble film surface, preventing fat globules from adsorbing and resulting in a discontinuous network of fat globules.

4. Conclusion

This study indicated that the addition of Ru could synergistically improve the foam stability of PP. It alleviated the drainage, disproportionation, and coalescence reactions of bubbles. The initial bubble size is considerably smaller, influenced by the PP/Ru mass ratio. As the mass ratio of PP/Ru remains at or below 64:4, the polyphenol binding equivalent increases progressively, while the particle size of PP/Ru complexes diminishes. The study of interfacial dilatational rheology and Interfacial shear rheology demonstrated that the synergistic interaction between PP and Ru facilitated the swift penetration of PP/Ru complexes into the air/water interface, thus enhancing the elastic strength of the foam system in both linear and nonlinear viscoelastic regions. As the PP/Ru mass ratio surpassed 64:4, the polyphenol binding equivalent decreased, leading to an increase in the particle size of the complexes. The air-water interface characteristics of PPI/Ru complexes were reversed, which hindered the formation of foam. After applying PP/Ru complexes to prepare low-fat cream, it was found that compared with PP alone, PP/Ru complexes effectively promoted the aggregation of fat globules in the cream. Promoted the formation of a dense and stable fat globule network structure. At the same time, the PP content distributed on the bubble membrane increases, which can effectively stabilize the bubble structure. When PP/Ru complexes replace 10 % of the fat, low-fat cream has higher structural strength and better stability. There is no significant difference in performance compared to full fat cream. In summary, this study provided a good idea for developing low-fat and low-calorie cream products.

CRediT authorship contribution statement

Chunyang Xia: Writing – original draft, Software, Conceptualization. **Fangxiao Lou:** Data curation. **Shuo Zhang:** Visualization. **Tianfu Cheng:** Methodology. **Zhaodong Hu:** Investigation. **Zengwang Guo:** Project administration, Funding acquisition. **Ping Ma:** Writing – original draft, Supervision, Conceptualization.

Declaration of competing interest

The authors declare that they have no known competing financial interests or personal relationships that could have appeared to influence the work reported in this paper.

Acknowledgements

Grants from Heilongjiang Province Specialty Discipline Project for the Production and Processing Advantages of Coarse Cereals (2022-78).

Data availability

Data will be made available on request.

References

Allen, K. E., Murray, B. S., & Dickinson, E. (2008). Development of a model whipped cream: Effects of emulsion droplet liquid/solid character and added hydrocolloid. *Food Hydrocolloids, 22*(4), 690–699. https://doi.org/10.1016/j.foodhyd.2007.01.017

Chen, X., Chen, Y., Zou, L., Zhang, X., Dong, Y., Tang, J., & Liu, W. (2019). Plant-based nanoparticles prepared from proteins and phospholipids consisting of a Core–multilayer-Shell structure: Fabrication, stability, and Foamability. *Journal of Agricultural and Food Chemistry, 67*(23), 6574–6584. https://doi.org/10.1021/acs.jafc.9b02028

Cheng, T., Wang, Z., Sun, F., Liu, H., Liu, J., Guo, Z., & Zhou, L. (2024). Gel properties of rice proteins-pectin composite and the delivery potential for curcumin: Based on different concentrations and the degree of esterification of pectin. *Food Hydrocolloids, 146*, Article 109305. https://doi.org/10.1016/j.foodhyd.2023.109305

Cheng, T., Zhang, G., Sun, F., Guo, Y., Ramakrishna, R., Zhou, L., & Wang, Z. (2024). Study on stabilized mechanism of high internal phase Pickering emulsions based on commercial yeast proteins: Modulating the characteristics of Pickering particle via sonication. *Ultrasonics Sonochemistry, 104*, Article 106843. https://doi.org/10.1016/j.ultsonch.2024.106843

Dai, S., Xu, T., Yuan, Y., Fang, Q., Lian, Z., Tian, T., & Wang, H. (2024). Combination and precipitation mechanism of soy protein and tea polyphenols. *Food Hydrocolloids, 146*, Article 109197. https://doi.org/10.1016/j.foodhyd.2023.109197

Dai, T., McClements, D. J., Hu, T., Chen, J., He, X., Liu, C., & Sun, J. (2022). Improving foam performance using colloidal protein–polyphenol complexes: Lactoferrin and tannic acid. *Food Chemistry, 377*, Article 131950. https://doi.org/10.1016/j.foodchem.2021.131950

Dickinson, E. (2017). Biopolymer-based particles as stabilizing agents for emulsions and foams. *Food Hydrocolloids, 68*, 219–231. https://doi.org/10.1016/j.foodhyd.2016.06.024

Fujii, S. (2024). Foams/bubbles stabilized with polymer particles. *Current Opinion in Colloid & Interface Science, 72*, Article 101808. https://doi.org/10.1016/j.cocis.2024.101808

Ghribi, A. M., Zouari, M., Attia, H., & Besbes, S. (2021). Study of protein / k-carrageenan mixture's effect on low-fat whipping cream formulation. *LWT, 147*, Article 111647. https://doi.org/10.1016/j.lwt.2021.111647

Goff, H. D. (1997). Instability and partial coalescence in Whippable dairy emulsions. *Journal of Dairy Science, 80*(10), 2620–2630. https://doi.org/10.3168/jds.S0022-0302(97)76219-2

Günal-Köroğlu, D., Lorenzo, J. M., & Capanoglu, E. (2023). Plant-based protein-phenolic interactions: Effect on different matrices and in vitro gastrointestinal digestion. *Food Research International, 173*, Article 113269. https://doi.org/10.1016/j.foodres.2023.113269

Guo, Y., Zhang, S., Gu, Y., Cheng, T., Sun, F., Wang, Y., & Guo, Z. (2025). Mechanism of sodium alginate synergistically improving foaming properties of pea protein isolate: Air/water interface microstructure and rheological properties. *Food Hydrocolloids, 159*, Article 110624. https://doi.org/10.1016/j.foodhyd.2024.110624

Han, L., Peng, X., Cheng, Y., Zhu, Y., Huang, Y., Zhang, S., & Qi, B. (2023). Effects of catechin types found in tea polyphenols on the structural and functional properties of soybean protein isolate–catechin covalent complexes. *LWT, 173*, Article 114336. https://doi.org/10.1016/j.lwt.2022.114336

Han, Y., Zhu, L., Qi, X., Zhang, H., & Wu, G. (2023). Characteristics of low-fat whipped cream containing protein-based fat replacers. *International Journal of Dairy Technology, 76*(2), 276–290. https://doi.org/10.1111/1471-0307.12934

Han, Y., Zhu, L., Zhang, H., & Wu, G. (2024). Fabrication and characterization of non-fat whipped cream analogue: Effects of type and concentration of polysaccharide. *International Journal of Biological Macromolecules, 276*, Article 133819. https://doi.org/10.1016/j.ijbiomac.2024.133819

Hotrum, N. E., Stuart, M. A. C., Vliet, T. V., Avino, S. F., & Van Aken, G. A. (2005). Elucidating the relationship between the spreading coefficient, surface-mediated partial coalescence and the whipping time of artificial cream. *Colloids and Surfaces A: Physicochemical and Engineering Aspects, 260*(1), 71–78. https://doi.org/10.1016/j.colsurfa.2005.03.004

Huang, D., Xu, Y., Zhang, W., Liu, Y., Zhang, T., Liu, H., & Li, D. (2024). Enhancement of foaming property of ormosia protein: Insights into the effect of high-intensity ultrasound on physicochemical properties and structure analysis. *Food Hydrocolloids, 152*, Article 109902. https://doi.org/10.1016/j.foodhyd.2024.109902

Huang, P., Huang, C., Ma, X., Gao, C., Sun, F., Yang, N., & Nishinari, K. (2021). Effect of pH on the mechanical, interfacial, and emulsification properties of chitosan microgels. *Food Hydrocolloids, 121*, Article 106972. https://doi.org/10.1016/j.foodhyd.2021.106972

Huyst, A. M. R., Van der Meeren, P., Housmans, J. A. J., Monge-Morera, M., Rousseau, F., Schymkowitz, J., & Delcour, J. A. (2023). Improved coalescence and creaming stability of structured oil-in-water emulsions and emulsion gels containing ovalbumin amyloid-like fibrils produced by heat and enzymatic treatments. *Food Hydrocolloids, 145*, Article 109142. https://doi.org/10.1016/j.foodhyd.2023.109142

Kontogiorgos, V., & Prakash, S. (2023). Adsorption kinetics and dilatational rheology of plant protein concentrates at the air- and oil-water interfaces. *Food Hydrocolloids, 138*, Article 108486. https://doi.org/10.1016/j.foodhyd.2023.108486

Li, X., Hu, Q., Jiang, S., Li, F., Lin, J., Han, L., & Chen, D. (2015). Flos Chrysanthemi Indici protects against hydroxyl-induced damages to DNA and MSCs via antioxidant mechanism. *Journal of Saudi Chemical Society, 19*(4), 454–460. https://doi.org/10.1016/j.jscs.2014.06.004

Liu, Z., Cao, Z., Zhao, M., Zhang, H., Wang, J., & Sun, B. (2022). Synergistic influence of protein particles and low-molecular-weight emulsifiers on the stability of a milk fat-based whippable oil-in-water emulsion. *Food Hydrocolloids, 127*, Article 107520. https://doi.org/10.1016/j.foodhyd.2022.107520

Mallamace, F., Corsaro, C., Mallamace, D., Vasi, S., Vasi, C., & Dugo, G. (2015). The role of water in protein's behavior: The two dynamical crossovers studied by NMR and FTIR techniques. *Computational and Structural Biotechnology Journal, 13*, 33–37. https://doi.org/10.1016/j.csbj.2014.11.007

Murray, B. S., Ventura, A., & Lallemant, C. (1998). Dilatational rheology of protein+non-ionic surfactant films at air–water and oil–water interfaces. *Colloids and Surfaces A: Physicochemical and Engineering Aspects, 143*(2), 211–219. https://doi.org/10.1016/S0927-7757(98)00256-8

Muse, M. R., & Hartel, R. W. (2004). Ice cream structural elements that affect melting rate and hardness. *Journal of Dairy Science, 87*(1), 1–10. https://doi.org/10.3168/jds.S0022-0302(04)73135-5

Najari, Z., Dokouhaki, M., Juliano, P., & Adhikari, B. (2024). Advances in the application of protein-polysaccharide-polyphenol ternary complexes for creating and stabilizing Pickering emulsions. *Future Foods, 9*, Article 100299. https://doi.org/10.1016/j.fufo.2024.100299

Niu, H., Wang, W., Dou, Z., Chen, X., Chen, X., Chen, H., & Fu, X. (2023). Multiscale combined techniques for evaluating emulsion stability: A critical review. *Advances in Colloid and Interface Science, 311*, Article 102813. https://doi.org/10.1016/j.cis.2022.102813

Rodríguez, S. D., von Staszewski, M., & Pilosof, A. M. R. (2015). Green tea polyphenols-whey proteins nanoparticles: Bulk, interfacial and foaming behavior. *Food Hydrocolloids, 50*, 108–115. https://doi.org/10.1016/j.foodhyd.2015.04.015

Sagis, L. M. C., & Fischer, P. (2014). Nonlinear rheology of complex fluid–fluid interfaces. *Current Opinion in Colloid & Interface Science, 19*(6), 520–529. https://doi.org/10.1016/j.cocis.2014.09.003

Sun, F., Li, Z., Kong, S., Ma, X., Liu, Y., & Yang, N. (2025). Linear and nonlinear interfacial rheology of responsive microgels at the oil-water interface. *Food Hydrocolloids, 158*, Article 110479. https://doi.org/10.1016/j.foodhyd.2024.110479

Tian, R., Han, X., Tian, B., Li, G., Sun, L., Tian, S., & Wang, S. (2023). Effects of covalent binding of different polyphenols on structure, rheology and functional properties of whey protein isolate. *LWT, 184*, Article 114968. https://doi.org/10.1016/j.lwt.2023.114968

Wang, Y., Dai, S., Lian, Z., Cheng, X., Tong, X., Wang, H., & Jiang, L. (2024). Polyphenol improve the foaming properties of soybean isolate protein: Structural, physicochemical property changes and application in angel cake. *International Journal of Biological Macromolecules, 277*, Article 134315. https://doi.org/10.1016/j.ijbiomac.2024.134315

Wang, Y., Liu, C., Lang, H., Hu, Z., Wang, X., Yang, Z., & Jiang, L. (2023). Effects of microwave on the structural and emulsifying properties and interfacial properties of oxidized soybean protein aggregates. *Food Chemistry: X, 19*, Article 100861. https://doi.org/10.1016/j.fochx.2023.100861

Wen, H., Zhang, D., Ning, Z., Li, Z., Zhang, Y., Liu, J., & Zhang, T. (2023). How do the hydroxyl group number and position of polyphenols affect the foaming properties of ovalbumin? *Food Hydrocolloids, 140*, Article 108629. https://doi.org/10.1016/j.foodhyd.2023.108629

Wu, J., Feng, W., Wang, R., Zhang, H., & Wang, T. (2023). Liquid foams with a lifetime of several days co-stabilized by monodisperse protein nanoparticles and mechanically stable starch nanocrystals. *Food Hydrocolloids, 145*, Article 109176. https://doi.org/10.1016/j.foodhyd.2023.109176

Wu, Y., Wu, Y., Xiang, H., Chen, S., Zhao, Y., Cai, Q., & Wang, Y. (2024). Emulsification properties and oil-water interface properties of l-lysine-assisted ultrasonic treatment in sea bass myofibrillar proteins: Influenced by the conformation of interfacial proteins. *Food Hydrocolloids, 147*, Article 109405. https://doi.org/10.1016/j.foodhyd.2023.109405

Xu, M., Du, Z., Liang, H., Yang, Y., Li, Q., Wan, Z., & Yang, X. (2021). Adsorption and foaming properties of edible egg yolk peptide nanoparticles: Effect of particle aggregation. *Current Research in Food Science, 4*, 270–278. https://doi.org/10.1016/j.crfs.2021.04.002

Ye, J., Deng, L., Wang, Y., McClements, D. J., Luo, S., & Liu, C. (2021). Impact of rutin on the foaming properties of soybean protein: Formation and characterization of flavonoid-protein complexes. *Food Chemistry, 362*, Article 130238. https://doi.org/10.1016/j.foodchem.2021.130238

Zhang, J., Cheng, T., Sun, M., Li, Y., Zhang, G., Hu, Z., & Wang, Z. (2024). Application of soy protein isolate-naringenin complexes as fat replacers in low-fat cream: Based on protein conformational changes, aggregation states and interfacial adsorption behavior. *International Journal of Biological Macromolecules, 274*, Article 133315. https://doi.org/10.1016/j.ijbiomac.2024.133315

Zhao, J., Xu, S., Gu, L., Yang, F., Fang, X., & Gao, S. (2024). High internal phase emulsions gels stabilized by soy protein isolate and rutin complexes: Encapsulation, interfacial properties and in vitro digestibility. *LWT, 203*, Article 116317. https://doi.org/10.1016/j.lwt.2024.116317